

## A uniformly cleaved epitaxially grown diamond crystal for synchrotron radiation

Armando H. Shinohara,<sup>a\*</sup> Mutsukazu Kamo<sup>b</sup> and Carlos K. Suzuki<sup>a</sup>

<sup>a</sup>UNICAMP - University of Campinas, Faculty of Mechanical Engineering, Department of Materials Engineering, CP6122, 13081-970, Campinas-SP, Brazil, and <sup>b</sup>NIRIM - National Institute for Research in Inorganic Materials, Namiki 1-1, Tsukuba, Ibaraki 305, Japan. E-mail: hideki@fem.unicamp.br

(Received 4 August 1997; accepted 13 January 1998)

A homoepitaxial single-crystal diamond (111) film grown by microwave-assisted chemical vapour deposition (CVD) and fractured along the [110] directions to form small triangles was investigated by X-ray double-crystal topography. The X-ray topographic image showed that all parts of the cleaved CVD diamond film sections uniformly reflected X-rays at the peak position of the rocking curve, which was measured in the Bragg case. Furthermore, no bending effect was observed and the CVD diamond film appeared to be more perfect than and showed higher integrated intensity than the natural diamond substrate.

**Keywords:** CVD single-crystal diamond film; cleavage lines; high integrated intensity.

### 1. Introduction

One of the major problems in X-ray optics for third-generation synchrotron radiation is the thermal deformation produced by the high heat load absorbed in the optical elements. To overcome this problem, a number of different crystal-cooling processes have been developed. Cryogenically and water-cooled optics for use with high-power synchrotron radiation beams have been suggested for mirrors (Rehn, 1985) and for crystal monochromators (Ishikawa, 1998; Marot, 1995; Smither, 1990; Bilderback, 1986). Single-crystal diamond is a well known material with very attractive thermal properties and a figure of merit  $\kappa/\alpha$  of the order of  $2 \times 10^7 \text{ W cm}^{-1}$  (depending on the type of diamond) compared with  $6 \times 10^5 \text{ W cm}^{-1}$  for silicon at room temperature. Diamond has a low atomic number and an absorption power lower than that of silicon. These merits have recently led X-ray optics scientists to evaluate and demonstrate the very high performance of diamond single crystals as high heat flux X-ray monochromators. Diamond single crystals of high crystalline perfection synthesized at high pressure and temperature have been used successfully at the APS (Mills, 1997), ESRF (Als-Nielsen *et al.*, 1994) and SPring-8 (Yamaoka *et al.*, 1995). However, high-quality diamond crystals larger than  $1 \text{ cm}^2$  are difficult to grow, limiting their application to undulator beam-lines (Freund, 1995; Yamaoka *et al.*, 1995). Another disadvantage of high-quality diamond crystals is the wavelength-integrated reflectivity of the 111 diamond reflection, which is about half that of silicon 111 (Blasdel *et al.*, 1990). For many X-ray scattering experiments, the narrow energy bandpass provided by a perfect

single-crystal monochromator is not necessary, but a high flux density is required (Deschamps *et al.*, 1995).

Recent progress in the growth of diamond films by chemical vapour deposition (CVD) has raised the hope of synthesizing large-area single-crystal diamond films. Furthermore, highly oriented CVD diamond films have been grown successfully on several kinds of substrates, such as silicon (Floter *et al.*, 1998; Jiang *et al.*, 1993; Geis *et al.*, 1991) or diamond (Posthill *et al.*, 1995; Kamo *et al.*, 1988); these are essentially II-a diamond and contain very low levels of impurity atoms.

In the present work, the results of a study of a uniformly cleaved homoepitaxially grown CVD single-crystal diamond (111) film by X-ray double-crystal topography are presented.

### 2. Experimental

The CVD single-crystal diamond film was homoepitaxially grown on one side of a natural diamond flattened parallel to the {111} planes using a gaseous mixture of hydrogen and methane under microwave glow discharge conditions of  $40 \text{ cm}^3 \text{ min}^{-1}$  for  $\text{CH}_4$  and  $0.12 \text{ cm}^3 \text{ min}^{-1}$  for  $\text{H}_2$ . The substrate quality was I-a; it was 3 mm wide, 4.5 mm long and 1.3 mm thick. The substrate was kept at 1153 K for a deposition run of 48 h. The thickness of the diamond film grown on it was estimated to be about 20  $\mu\text{m}$  from the run time. The sample was prepared at NIRIN, National Institute for Research in Inorganic Materials, Tsukuba, Japan (Nakazawa *et al.*, 1987). The diamond film spontaneously cleaved into small triangular sections with edges along the [110] directions and with {111} cleavage planes resulting from high strain and lattice mismatch at the film–substrate interface, and the presence of impurities and structure defects (Suzuki *et al.*, 1998; Tarutani *et al.*, 1996; Nakazawa *et al.*, 1987). Fig. 1 shows the uniformly cleaved (111) film extending along the whole sample. Furthermore, an epitaxially grown diamond film was also observed on the lateral faces of the substrate, with cleavage lines running along the [110] directions.

The recording of the rocking curves and the topographic imaging were carried out with a ‘quasi-parallel’ (+, –) double-crystal arrangement of Si(220) and diamond (111) using the Bragg case and Cu  $K\alpha$  radiation from a fine-focus sealed-off

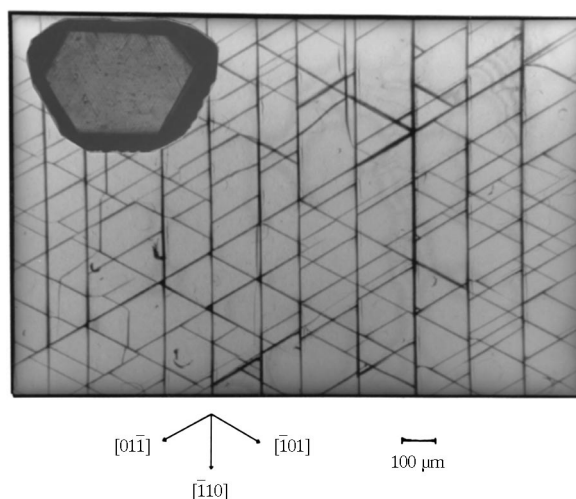


**Figure 1**  
The epitaxial CVD single-crystal diamond film uniformly cleaved into triangular sections. The inset image is the natural diamond substrate with the diamond film on it.

X-ray tube. The Si(220) monochromator used had an asymmetry factor  $1/b \approx 5$ . The interplanar spacings for silicon and diamond were 1.920 and 2.059 Å, respectively, giving a difference of 7.2%. This arrangement is slightly dispersive, but good enough to improve the topographic imaging sensitivity to micro-strain order in the crystalline lattice. The X-ray generator and data-acquisition system of the Rigaku Dmax 2200 series coupled with a high-precision KTG-11P Kohzu Seiki goniometer were used. A schematic diagram of the ‘quasi-parallel’ X-ray double-crystal topography arrangement is shown in Fig. 2.

**3. Results and discussion**

Fig. 3 shows the rocking curve of the diamond film plus substrate obtained with the X-ray beam illuminating the whole surface area. The full width at half-maximum (FWHM) of the film plus substrate (80 arcsec) was about three times larger than for the substrate (26 arcsec), even though partial stress relaxation had occurred because of the fracture of the film.

When the X-ray absorption of the sample is low, two effects can occur: an asymmetric broadening and a shift of the measured peak positions because diffraction also takes place in the interior of the sample (Keating & Warren, 1952). The measurement of the X-ray diffraction profile with the angular precision of the Dmax-2200 goniometer (precision of 1/1000°) showed no detectable angular shift. Therefore, if an angular shift exists, it should be smaller than 4 arcsec. Furthermore, according to the extinction thickness,  $t_e$ , the crystal thickness needed to fully diffract the X-ray, *i.e.* for which the peak reflectivity is close to (~95% of) its maximum value, can be estimated for the symmetric Bragg case by

$$t_e = v_o / (2d_{(111)} r_o F_{Hr} C) \tag{1}$$

where  $v_o$  is the volume of the crystallographic unit cell,  $d_{(111)}$  is the lattice spacing of the diffraction planes in the (111) direction,  $r_o$  is the classical electron radius,  $F_{Hr}$  is the real part of the structure factor and  $C$  is the polarization factor. The estimated value of the extinction thickness is  $t_e \approx 2.2 \mu\text{m}$  (Freund, 1995). However, the X-ray double-crystal topographic setting used in the present investigation is slightly dispersive and can contribute to a small increase in rocking-curve broadening. In order to estimate the contribution of the diamond film correcting the slight dispersion of the X-ray double-crystal topographic setting and the substrate effects for the broadening of the rocking-curve profile, the Warren (1941) method was applied according to the equation

$$B_{\text{film}}^2 = B_{\text{film+instrument}}^2 - B_{\text{substrate+instrument}}^2 \tag{2}$$

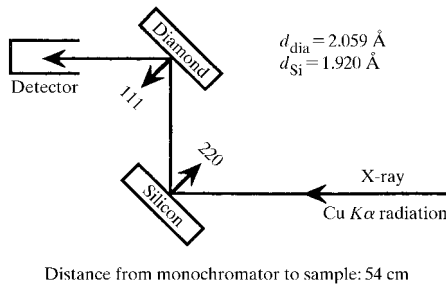


**Figure 2**  
A schematic diagram of the double-crystal X-ray topography experiment.

The  $B_{\text{film}}$  value estimated by this method is 75 arcsec. In this evaluation, the FWHM of the rocking curve of the side of the substrate opposite the side on which the the diamond films were grown was used. Broadening as a result of particle-size effects is negligible as the fractured regions are much bigger than 100 μm

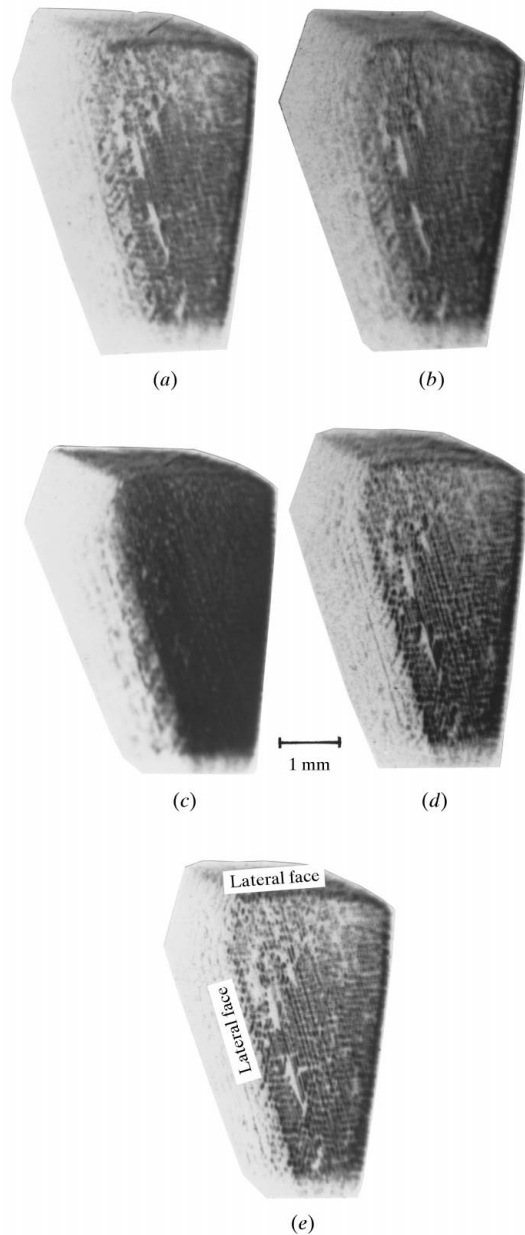
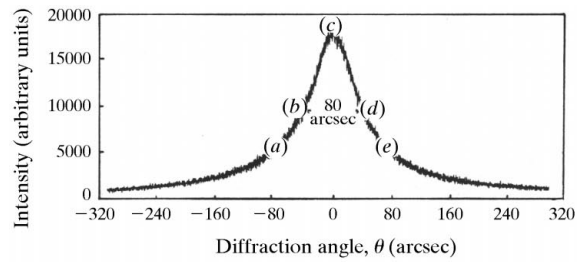


**Figure 3**  
The rocking curve and X-ray topographs of the CVD diamond film plus substrate recorded at five angular positions.

(Cullity, 1978). The integrated intensity from the CVD diamond film, normalized by the effective area, was three times larger than from the substrate. Therefore, the biggest effect contributing to the broadening of the rocking-curve profile is the residual stress generated by the presence of impurities and defects in the CVD diamond film (Suzuki *et al.*, 1998; Tarutani *et al.*, 1996).

The X-ray topographic image obtained at the peak position of the rocking curve (Fig. 3c) showed high uniform reflectivity in comparison with the images shown in Figs. 3(a), 3(b), 3(d) and 3(e), recorded at the angular positions indicated on the rocking curve. This image shows that the crystallographic orientation of each section of CVD diamond film is very similar, even though the diamond film is cleaved along the whole surface. This topograph also showed that the sample is not bent (at least in a range up to a few arcsec).

The crystalline quality of the fractured regions of about 100  $\mu\text{m}$  was studied by plane-wave X-ray topography using a highly asymmetric Si(111) monochromator ( $1/b \simeq 20$ ). It was possible to separate the diffraction peaks of the (111) epitaxial CVD single-crystal diamond film from the substrate. The higher diffraction angle of the CVD film ( $\Delta\theta = 65$  arcsec) compared with the substrate shows that the  $d$  spacing of the film is smaller than the  $d$  spacing of the substrate along the [111] direction. This result indicates that the CVD single-crystal diamond film is more perfect than the substrate.

#### 4. Conclusions

A uniformly cleaved CVD (111) diamond film grown on natural diamond flattened parallel to the (111) plane was investigated by X-ray double-crystal topography. Even though the whole diamond film is fractured into small triangles ( $\sim 100 \mu\text{m}$ ), all these small sections uniformly diffract X-rays at the peak position of the rocking curve measured in the Bragg case. Furthermore, the integrated intensity of X-ray diffraction by the film was about three times larger than that by the diamond substrate. Since many X-ray scattering experiments using synchrotron radiation do not require a narrow energy bandpass, CVD epitaxial single-crystal diamond is proposed to be a useful optical component for third-generation synchrotron radiation. The growth of large single-crystal diamond films of high quality and of desired thickness on different kinds of substrates by CVD has made progress and has yielded quite good results. At present, 3 in CVD single-crystal

diamond films can be grown and this is expected to increase to 6 to 8 in using heteroepitaxial processes in the future.

We would like to express our thanks to Dr M. Yamamoto, The Institute of Physical and Chemical Research (RIKEN), for valuable comments and fruitful discussions. The technical assistance of T. Tagurti (Rigaku Corp.), M. S. Tanaka and P. H. Godoy is highly appreciated. The financial support received from CNPq and FAPESP is gratefully acknowledged.

#### References

- Als-Nielsen, J., Freund, A. K., Grubel, G., Linderholm, J., Nielsen, M., Sanchez del Rio, M. & Sellschop, J. P. F. (1994). *Nucl. Instrum. Methods Phys. Res.* **B94**, 306–318.
- Bilderback, D. H. (1986). *Nucl. Instrum. Methods*, **A246**, 434–436.
- Blasdel, R. C., Assoufid, L. A., & Mills, D. M. (1990). *A Diamond Monochromator for APS Undulator-A Beamlines*. Report ANL/APS/TB-24. Argonne National Laboratory, Argonne, USA.
- Cullity, B. D. (1978). *Elements of X-ray Diffraction*, ch. 9. Reading, MA: Addison-Wesley.
- Deschamps, P., Engstrom, P., Fiedler, S., Riekel, C., Wakatsuki, S., Hoghoj, P. & Ziegler, E. (1995). *J. Synchrotron Rad.* **2**, 124–131.
- Floter, A., Guttler, H., Schulz, G., Steinbach, D., Zachai, R., Bermaier, A. & Dollinger, G. (1998). *Diam. Relat. Mater.* **7**, 283–288.
- Freund, A. K. (1995). *Opt. Eng.* **34**, 432–440.
- Geis, M. W., Smith, H. I., Argoitia, A., Angus, J., Ma, G.-H. M., Glass, J. T., Butler, J., Robison, C. J. & Pryor, R. (1991). *Appl. Phys. Lett.* **58**(22), 2485–2487.
- Ishikawa, T. (1998). *SRI97 Meeting*, Abstract 5MO2.
- Jiang, X., Klages, C.-P., Zachai, R., Hartweg, M. & Fusser, H.-J. (1993). *Appl. Phys. Lett.* **62**(26), 3438–3440.
- Kamo, M., Yurimoto, H. & Sato, Y. (1988). *Appl. Surf. Sci.* **33/34**, 553–560.
- Keating, D. T. & Warren, B. E. (1952). *J. Appl. Phys.* **23**(10), 519–522.
- Marot, G. (1995). *Opt. Eng.* **34**, 426–431.
- Mills, D. M. (1997). *J. Synchrotron Rad.* **4**, 117–124.
- Nakazawa, H., Kanazawa, Y., Kamo, M. & Osumi, K. (1987). *Thin Solid Films*, **151**, 199–206.
- Posthill, J. B., Malta, D. P., Hudson, G. C., Thomas, R. E., Humphreys, T. P., Hendry, R. C., Rudder, R. A. & Markunas, R. J. (1995). *Thin Solid Films*, **271**, 39–49.
- Rehn, V. (1985). *SPIE J.* **582**, 238–250.
- Smither, R. K. (1990). *Nucl. Instrum. Methods Phys. Res.* **A291**, 286–299.
- Suzuki, C. K., Shinohara, A. H., Godoy, P. H., Watanabe, N. & Kamo, M. (1998). *Diam. Relat. Mater.* **7**, 289–292.
- Tarutani, M., Takai, Y., Shimizu, R., Ando, T., Kamo, M. & Bando, Y. (1996). *Appl. Phys. Lett.* **68**(15), 2070–2072.
- Warren, B. E. (1941). *J. Appl. Phys.* **12**, 375–383.
- Yamamoto, M., Kumasaka, T., Fujisawa, T. & Ueki, T. (1998). *J. Synchrotron Rad.* **5**, 222–225.
- Yamaoka, H., Ohtomo, K. & Ishikawa, T. (1995). *Rev. Sci. Instrum.* **66**(2), 2116–2118.